Phytopathology Research

RESEARCH

Open Access

The effector Fg62 contributes to *Fusarium graminearum* virulence and induces plant cell death

Shuchen Wang[1,2,3†], Sen Yang[1,2,3†], Kaixin Dai[1,2,3], Wenyue Zheng[1,2,3], Xiaoyi Zhang[1,2,3], Bo Yang[1,2,3,4*], Wenwu Ye[1,2,3], Xiaobo Zheng[1,2,3] and Yuanchao Wang[1,2,3*]

Abstract

Although the functions of most protein effectors secreted by fungi are not predictable, they are known to modulate host immunity and facilitate infection. *Fusarium graminearum* is one of the 10 most abundant plant pathogenic fungi worldwide. To date, few effector proteins secreted by *F. graminearum* have been identified. In this study, we screened a putative effector protein Fg62 from proteins that contain signal peptides and unknown functional domains in *F. graminearum* secretome. *Fg62* expression was highly upregulated during the early stages of *F. graminearum* infection, and its deletion reduced *F. graminearum* virulence in wheat and soybean. Transient expression of Fg62 or the recombinant protein led to plant cell death in *Nicotiana benthamiana*, and the signal peptide of Fg62 was required for cell death activation. Fg62 homologs are distributed in two species of the *F. sambucinum* species complex, which are also able to induce cell death in *N. benthamiana*. Fg62 activated plant immunity by increasing the expression of defense-related genes, and the recombinant Fg62 protein induced plant resistance to various pathogens. Overall, our results revealed that the extracellular effector Fg62 contributes to both pathogen virulence and plant immunity induction, providing new avenues for the development of environmentally friendly crop disease control strategies utilizing non-polluting immune-inducing factors.

Keywords *Fusarium graminearum*, Cell death, Fg62, Effector, Plant immunity

Background

Fusarium graminearum is one of the 10 most abundant plant pathogenic fungi worldwide (Dean et al. 2012), causing devastating Fusarium head blight (FHB) infection in wheat and Gibberella ear rot in maize (Starkey et al. 2007; Yulfo-Soto et al. 2022). *F. graminearum* colonizes soybean and is responsible for soybean root rot (Pioli et al. 2004; Ye et al. 2020). The mycotoxin deoxynivalenol (DON) and its derivatives are also produced by *F. graminearum* in infected plants, representing a serious health risk to humans and livestock (Audenaert et al. 2013). Due to soybean-wheat rotation, maize-soybean intercropping, and straw returning management practices, *F. graminearum* appears to be a growing hazard to agricultural production (Broders et al. 2007; Chang et al.

†Shuchen Wang and Sen Yang have contributed equally to this work

*Correspondence:
Bo Yang
yangb@njau.edu.cn
Yuanchao Wang
wangyc@njau.edu.cn
[1] Department of Plant Pathology, Nanjing Agricultural University, Nanjing 210095, China
[2] Key Laboratory of Plant Immunity, Nanjing Agricultural University, Nanjing 210095, China
[3] Key Laboratory of Soybean Disease and Pest Control (Ministry of Agriculture and Rural Affairs), Nanjing Agricultural University, Nanjing 210095, China
[4] College of Grassland Science, Nanjing Agricultural University, Nanjing 210095, China

2018). Germplasm with complete resistance or immunity to *F. graminearum* is lacking. As such, it is difficult to control the diseases caused by this pathogen. To date, two FHB resistance genes *Fhb1* and *Fhb7* have been cloned and characterized at the molecular level (Li et al. 2019; Su et al. 2019; Wang et al. 2020). Therefore, further elucidation of the mechanisms by which *F. graminearum* interacts with plants is crucial for its control.

Fungal pathogens use diverse biotrophic strategies to invade plant immune surveillance, and they secrete a considerable range of effector proteins to achieve successful colonization (Giraldo and Valent 2013). Fungal effector proteins are small secreted proteins containing fewer than 300 amino acids (Duplessis et al. 2011; Zuccaro et al. 2011). Many of these proteins are rich in cysteine (2–20%), and their tertiary structures are stabilized by disulfide bridges (Stergiopoulos et al. 2013). Fungal effector proteins are mainly secreted through the endoplasmic reticulum-Golgi apparatus route, which they can only enter host cells if they contain an N-terminal secretion signal (Stergiopoulos and de Wit 2009; Giraldo and Valent 2013). Unlike bacterial or oomycete pathogens, most fungal-secreted protein effectors appear to have no predictable function (Presti et al. 2015). In past decade, only a few such proteins have been found to simultaneously influence *F. graminearum* virulence and manipulate plant immunity. *FGL1* encodes a secreted lipase that can release free fatty acids to inhibit plant innate immunity-related callose accumulation during infection (Voigt et al. 2005). FgNahG is a secreted salicylate hydroxylase that coverts salicylic acid into catechol and plays an important role in virulence (Qi et al. 2019). The secreted protein Osp24 competes with TaFROG protein for binding with TaSnRK1α kinase, regulating basal plant defense against pathogens (Jiang et al. 2020). The ribonuclease secretion protein Fg12 contributes to virulence and induces plant cell death (Yang et al. 2021). A small secreted protein, Fg02685 in *F. graminearum*, enhances broad-spectrum disease resistance in plants, whereas its knockout mutation reduces the growth and development of *Fusarium* in wheat spikes (Xu et al. 2022).

Plants have a complex, multilayered immune system that is challenged by natural coevolution among pathogens. Plants rely on pattern recognition receptors (PRRs) to recognize conserved microbial features including pathogen-associated molecular patterns (PAMPs) or damage-associated molecular patterns to activate PAMP-triggered immunity (PTI) (Boller and Felix 2009; Couto and Zipfel 2016). In turn, pathogens have also employed numerous effectors to establish successful infections during the coevolution of hosts and microbes. In plants, effectors are also recognized by intracellular nucleotide binding-domain, leucine-rich, repeat-containing receptors (NLRs), and subsequently lead to robust effector-triggered immunity (ETI) (Jones and Dangl 2006). Signaling initiated by PRRs and NLRs leads to overlapping downstream cellular responses, including the expression of defense-related genes, a burst of reactive oxygen species (ROS) production, and callose deposition (Tsuda and Katagiri 2010; Peng et al. 2018). In contrast to the previous opinion that PTI and ETI are independent from each other, recent evidences have indicated complex crosstalk between them (Ngou et al. 2021; Pruitt et al. 2021; Yuan et al. 2021a, b). The exploitation of induced plant resistance could provide an alternative strategy for controlling crop diseases.

In this study, we examined the ability of candidate effector proteins containing signal peptides and unknown functional domains from the *F. graminearum* secretome to trigger plant cell death, and further characterized the extracellular effector Fg62, which induces cell death. Fg62 not only contributes to the pathogenicity of *F. graminearum*, but also function as a plant immune inducer that could enhance disease resistance against oomycetes and filamentous fungal pathogens.

Results

Fg62 induces cell death in *Nicotiana benthamiana*

A previous study has analyzed the secretome of *F. graminearum* PH-1 using liquid chromatography-tandem mass spectrometry (LC–MS/MS), and identified 72 proteins (Yang et al. 2021). To further investigate the function of *F. graminearum*-secreted proteins, we identified 12 candidate proteins containing signal peptides and unknown conserved domains. They are potential effector proteins, including six apoplastic proteins and six non-apoplastic proteins, based on their localization prediction by the ApoplastP machine learning model. We cloned the full-length coding sequences of eight candidate proteins into the binary PVX-based vector pGR107 for further transient expression in *N. benthamiana* leaves by agroinfiltration (Additional file 1: Table S1). PsXEG1 was used as a positive control. The results showed that the apoplastic secreted protein Fg62 induced plant cell death (Fig. 1a). Compared to green fluorescent protein (GFP), a significant change in electrolyte leakage was observed in the region infiltrated by Fg62 (Fig. 1b).

The open reading frame of *Fg62* (FGSG_13412) is a 534 bp sequence encoding a 177-amino acid protein and containing seven cysteine residues. Amino acids 1–19 are predicted to be a secretory signal peptide (SP) using the Signal IP 5.0 server, and the remaining residues contained no known functional domains. These features are similar to the general characteristics of fungal effector proteins (Stergiopoulos and de Wit 2009; Giraldo and Valent 2013). No transmembrane helices of Fg62 were

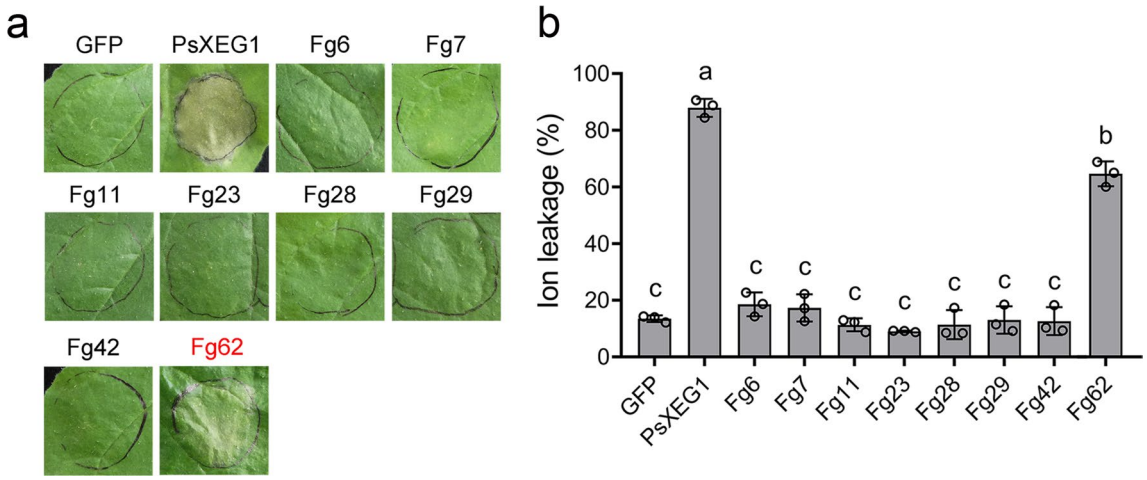

Fig. 1 Fg62 induced cell death in *Nicotiana benthamiana*. **a** Cell death detection on *N. benthamiana* leaves after transient expression of eight candidate effectors, green fluorescent protein (GFP), and PsXEG1. Candidate proteins were derived from the secretome of *Fusarium graminearum* PH-1 and possessed signal peptides and unknown functional domains. Representative images were taken at 7 days post-inoculation (dpi). **b** Quantification of cell death by electrolyte leakage measurement. Electrolyte leakage from infiltrated leaf discs was measured as a percentage of leakage from boiled discs. Means and standard errors (SEs) of three independent experiments are shown. Different letters above the bars indicate significant differences according to one-way analysis of variance (ANOVA), followed by Tukey's test ($P < 0.05$)

found, suggesting that the protein is likely secreted into the extracellular space.

Fg62 expression is upregulated during the early stages of *F. graminearum* infection

To investigate the potential roles of Fg62, we inoculated etiolated soybean hypocotyls and wheat leaves with fresh *F. graminearum* mycelium and collected samples at different time points. Using quantitative reverse-transcription polymerase chain reaction (qRT-PCR) analysis, we found that *Fg62* expression was upregulated in both wheat and soybean at 2 h post-infection (hpi), peaked at 4 hpi, and then gradually decreased (Fig. 2). Thus, *Fg62* expression was strongly induced during the early stages of infection.

Fg62 contributes to the virulence of *F. graminearum*

To assess the importance of Fg62 in the virulence of *F. graminearum*, we generated *Fg62* gene-deleted mutants (Additional file 2: Figure S1). Further

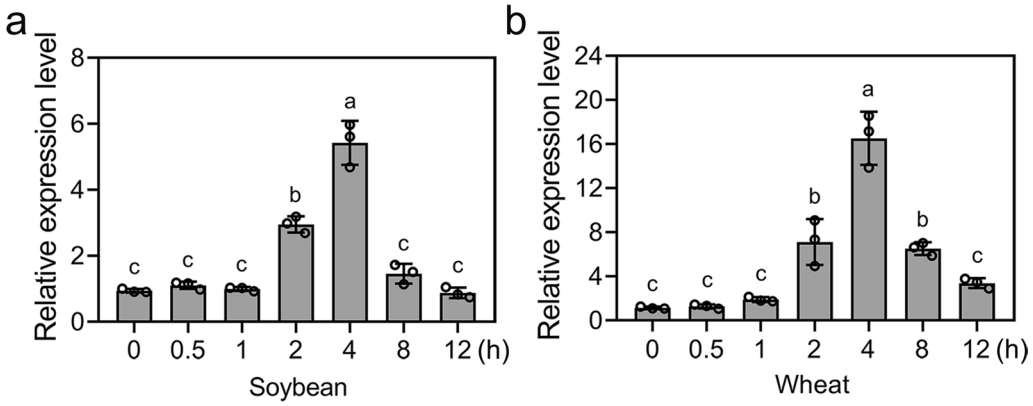

Fig. 2 *Fg62* expression was upregulated at the early stage of *Fusarium graminearum* infection. **a** Relative transcript levels of *Fg62* during different stages of *F. graminearum* infection in soybean. Etiolated soybean hypocotyls inoculated with *F. graminearum* PH-1 fresh mycelium were harvested at 0, 0.5, 1, 2, 4, 8, and 12 h post-inoculation (hpi). **b** Relative transcript levels of *Fg62* during different stages of infection in wheat. Wheat leaves were pre-wounded. Data are the means of three independent experiments. Different letters above the bars indicate significant differences (one-way ANOVA, Tukey's test; $P < 0.05$)

phenotypic characterization showed that the growth rate, colony morphology, sensitivity to multiple stresses and DON production of three Fg62-deletion mutants (Δ*Fg62*-M1, M2, and M3) were not significantly different from those of the wild-type (WT) strain PH-1 (Additional file 2: Figures S2, S3 and Additional file 1: Table S2). However, compared to WT strains, Δ*Fg62* mutants caused less severe symptoms on soybean hypocotyls, and the biomass of Δ*Fg62* mutants was lower than WT strains (Fig. 3a, b). Next, we used a wheat coleoptile infection system to perform a more detailed analysis of the deletion strains. When wounded coleoptiles of 3-day-old susceptible wheat seedlings (NJ58) were inoculated with conidia, Δ*Fg62* mutants induced shorter lesions than WT strains at 7 days post-inoculation (dpi) (Fig. 3c, d).

To confirm that the reduced virulence observed in mutants resulted from the deletion of *Fg62*, we complemented the mutant with a WT Fg62-GFP fusion construct under the control of its native promoter, and obtained complement mutants (Δ*Fg62*-C1, C2). The pathogenicity defects of Δ*Fg62* were compensated by genetic complementation (Fig. 3).

Signal peptide is required for Fg62-induced cell death

To determine which domain is responsible for Fg62 cell death-inducing effects, we constructed a signal peptide (amino acids 1–19)-deleted mutant (Fg62-nsp), and transiently expressed it in *N. benthamiana.* Fg62-nsp did not induce cell death in *N. benthamiana* (Fig. 4a, b), suggesting that the cell death-inducing effects of Fg62 depend on a signal peptide. Immunoblotting analysis confirmed the presence of Fg62 in infiltrated leaves (Fig. 4c).

The Fg62 signal peptide was tested using yeast signal trap assay to validate the secretory function. The yeast YTK12 strain carrying pSUC2-Fg62SP and the positive control pSUC2- Avr1bSP (Avr1b signal peptide) was able to grow on CMD-W and YPRAA, indicating that the Fg62 signal peptide had a secretion function. The enzyme activities of the secreted invertase from the transformants were also detected in vivo. 2,3,5-triphenyl tetrazolium chloride was converted into the insoluble red-colored 1,3,5-triphenyl formazan after adding yeast containing Avr1bSP or Fg62SP, indicating that invertase was secreted from the yeast in the presence of the Fg62 signal peptide (Fig. 4d).

The entire length of Fg62 and Fg62-nsp tagged with GFP were used to detect the localization in *N. benthamiana* after NaCl-induced plasmolysis to further confirm

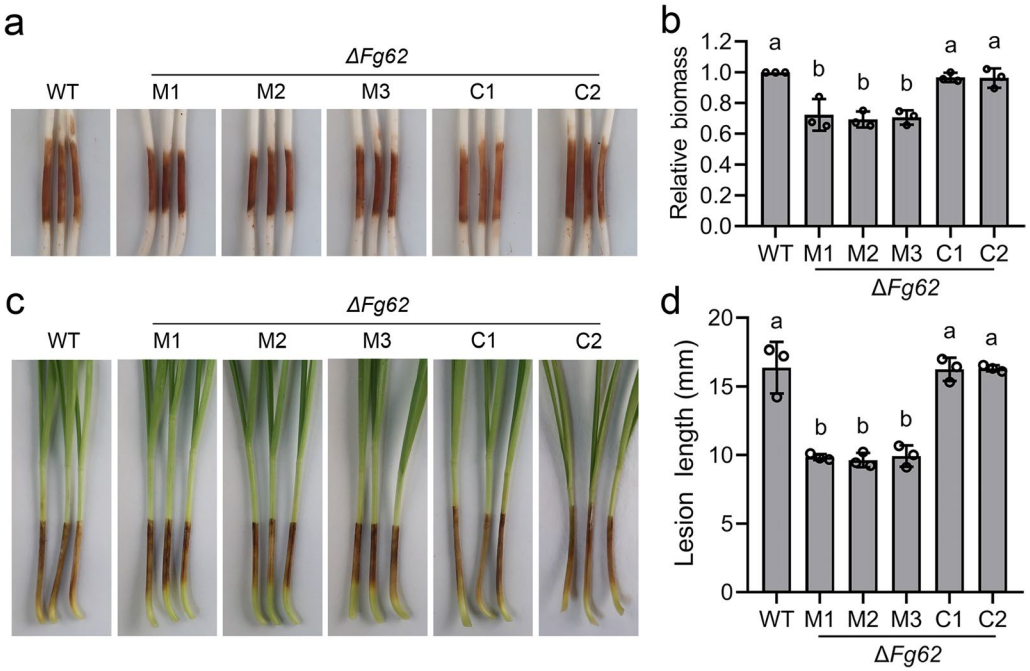

Fig. 3 Fg62 contributes to the virulence of *Fusarium graminearum*. **a** Representative image of lesions on etiolated soybean hypocotyls at 3 days post-inoculation (dpi). **b** *F. graminearum* biomass was determined by qRT-PCR. Means and SEs from three biological replicates are shown. **c** Symptoms on wheat coleoptiles at 7 dpi with the indicated strain. **d** Lesion lengths on wheat coleoptiles after inoculation with the indicated strains. Means and SEs from three biological replicates are shown, each using nine wheat plants. WT: wild-type PH-1; M1, M2, M3: independent Fg62-deletion mutants; C1, C2: independent complemented strains of Fg62 gene deletion mutants. Different letters above the bars indicate significant differences (one-way ANOVA, Tukey's test; $P < 0.05$)

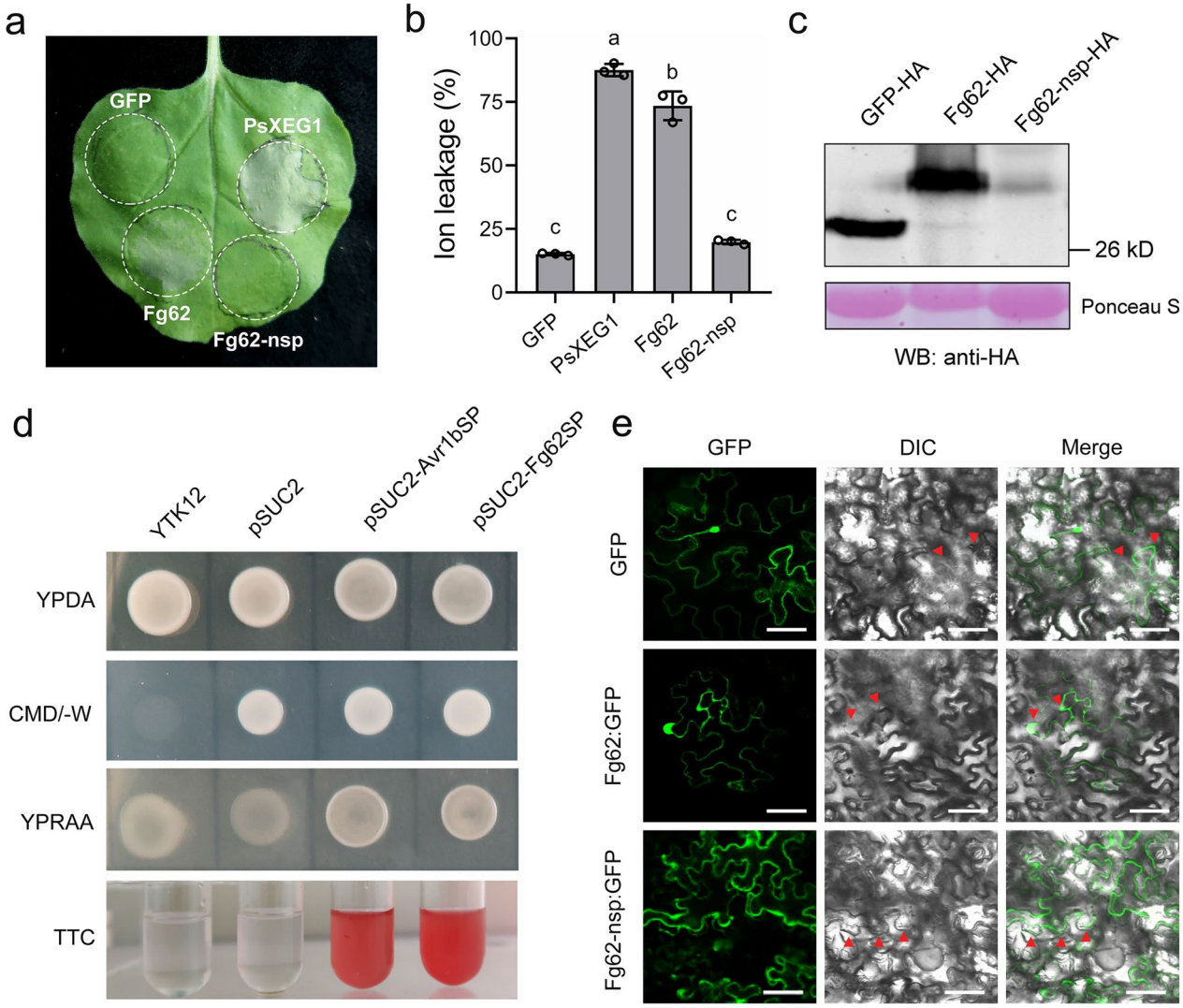

Fig. 4 Functional evaluation of Fg62 signal peptide. **a** Cell death detection on *Nicotiana benthamiana* leaves after transient expression of Fg62, Fg62-nsp, GFP, and PsXEG1. Representative images were taken at 7 days post-inoculation (dpi). **b** Detection of electrolyte leakage in *N. benthamiana* leaves transiently expressing Fg62, Fg62-nsp, GFP, and PsXEG1 at 7 dpi. Different letters above the bars indicate significant differences (one-way ANOVA, Tukey's test; $P < 0.05$). **c** Representative immunoblots showing the protein levels of Fg62 and Fg62-nsp, all fused with HA tags and transiently expressed in *N. benthamiana* leaves. Ponceau S staining indicates equal loading. **d** Functional validation of Fg62 signal peptide. The indicated strains were grown on YPDA, CMD-W, or YPRAA medium for 2 days. The invertase enzymatic activity was detected by reducing 2,3,5-triphenyl tetrazolium chloride (TTC) to insoluble red-colored 1,3,5-triphenyl formazan. **e** These full-length Fg62 and Fg62-nsp tagged with GFP and GFP alone were transiently expressed in *N. benthamiana*. Plant cells were treated with 70 mM NaCl for plasmolysis and analyzed by confocal microscopy at 36 h after *Agrobacterium* infiltration. The asterisk indicates the apoplast region (bars = 50 μm)

the function of the Fg62 signal peptide. The fluorescence signals of Fg62:GFP were observed in *N. benthamiana* apoplast, while fluorescence signals of cells expressing GFP alone and Fg62-nsp:GFP were not observed (Fig. 4e).

Fg62 is conserved in the *F. sambucinum* species complex

To study the phylogenetic distribution of Fg62 homologs in different microbes, we mined the genomes and the predicted protein sequences of three oomycete (*Phytophthora sojae*, *P. infestans*, and *Pythium ultimum*), two bacterial (*Pseudomonas syringae* and *Xanthomonas oryzae*), and 14 fungal species. We found no significant matches (> 10% similarity) among oomycete or bacterial pathogens (data not shown), and no sequence similar to Fg62 was found in the *F. graminearum* genome. Comprehensive phylogenetic analysis divided the 14 fungal species into three groups. We found one homologous sequence to Fg62 in each of *F.*

culmorum and *F. pseudograminearum*, but only partially similar proteins in other *Fusarium* species or fungi (Fig. 5a).

We randomly selected two fungal species from each of the three groups, and then cloned the full-length coding sequences into a vector and conducted transient expression by agroinfiltration in *N. benthamiana* leaves. Similar to Fg62, we found that only Fg62 homologs from *F. culmorum* and *F. pseudograminearum* induced cell death in *N. benthamiana* (Fig. 5b). Cell death induction was also monitored using ion leakage, which showed consistent results (Fig. 5c). *F. culmorum* and *F. pseudograminearum* belong to the same *F. sambucinum* species complex as *F. graminearum* (Ma et al. 2013; O'Donnell et al. 2013). These results suggest that Fg62 is conserved in species related to *F. graminearum*.

Fg62 enhances disease resistance in *N. benthamiana*

To further confirm the plant cell death-inducing effects of Fg62, we obtained recombinant Fg62 protein through a prokaryotic expression system (Additional file 2: Figure S4).

To understand the plant immunity-eliciting activity of Fg62, we investigated its ability to induce disease resistance. We sprayed 1 μM Fg62 recombinant protein on the whole *N. benthamiana* plants, and then inoculated *Phytophthora capsici* onto leaves after 72 h treatment. At 36 hpi, the area of *P. capsici* infection on leaves treated with Fg62 was significantly reduced compared to blank control BSA (bovine serum albumin), indicating that Fg62 had induced *N. benthamiana* resistance to *P. capsici* (Fig. 6a). The RT-PCR results showed that Fg62 inhibited *P. capsici* infection, with a biomass reduction of approximately 50% compared to the control (Fig. 6b).

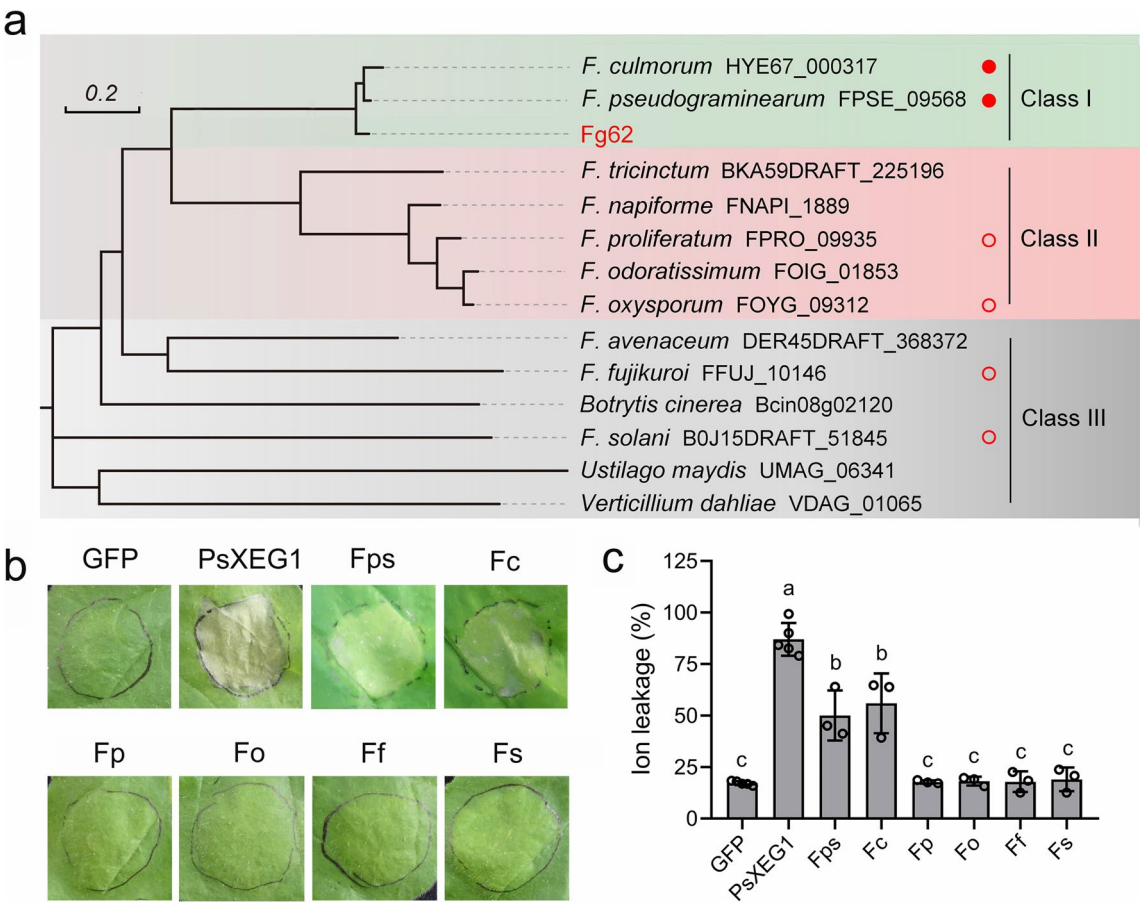

Fig. 5 Fg62 is conserved in the *Fusarium sambucinum* species complex. **a** Phylogenetic tree of Fg62 and 14 related sequences from different fungal species. **b** Fg62 homologs from *F. culmorum* and *F. pseudograminearum* induced cell death in *Nicotiana benthamiana*. Representative photographs were taken at 7 days post-inoculation (dpi). **c** Quantification of cell death by electrolyte leakage measurement. Means and SEs from three independent experiments are shown. Different letters above the bars indicate significant differences (one-way ANOVA, Tukey's test; $P < 0.05$). Fc, *F. culmorum*; Ff, *F. fujikuroi*; Fo, *F. oxysporum*; Fp, *F. proliferatum*; Fps, *F. pseudograminearum*; Fs, *F. solani*

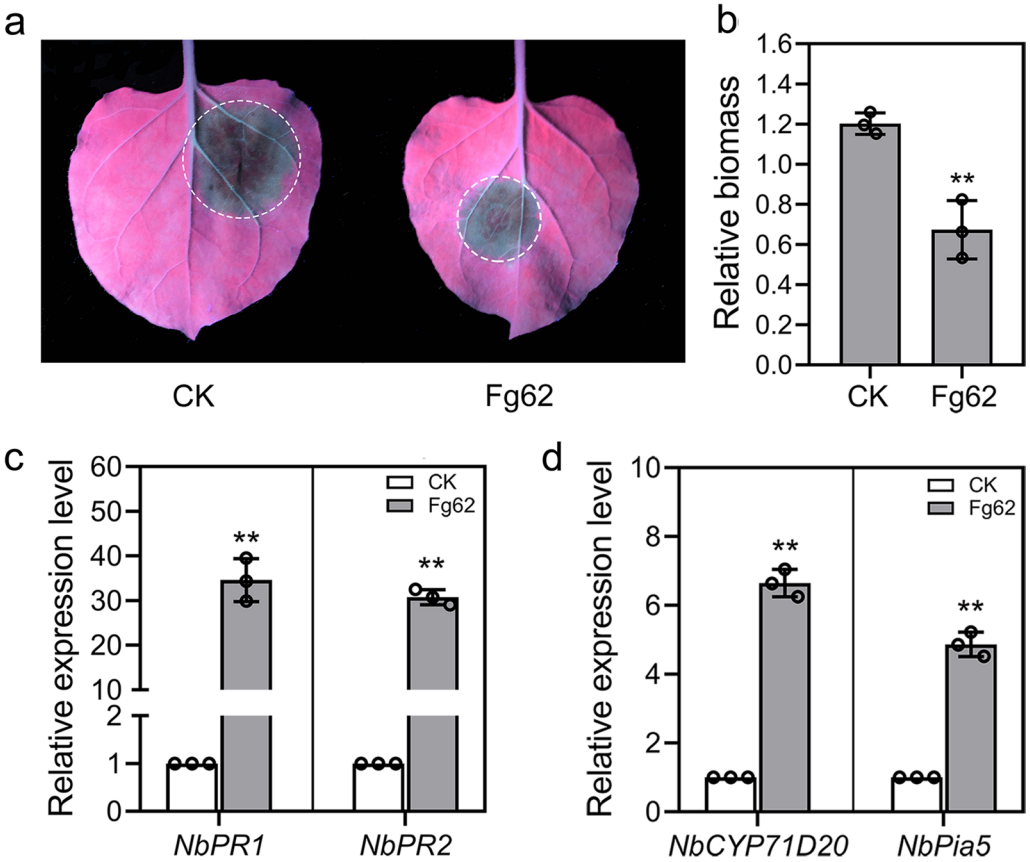

Fig. 6 Fg62 induces plant immunity in *Nicotiana benthamiana*. **a** Representative photographs of disease spots induced by *Phytophthora capsici* on *N. benthamiana* leaves. *N. benthamiana* leaves were pre-sprayed with proteins and inoculated with 5 mm diameter hyphal blocks of *P. capsici* 72 h later. Leaves were photographed under ultraviolet light at 30 h post-inoculation (hpi). **b** Relative biomass of *P. capsici* under different treatments in **a**. **c**, **d** Relative transcript levels of four plant defense-related marker genes in *N. benthamiana* after 72 h treated with the indicated proteins. Means and SEs from three independent experiments are shown. Asterisks indicate significant differences from the control based on Student's *t*-test

Fg62 triggers plant immunity responses in *N. benthamiana*

To determine whether Fg62 could activate plant defense responses, we investigated the expression of several defense-related genes in *N. benthamiana* leaves after 72 h infiltration with 1 μM of recombinant protein. qRT-PCR analysis showed that Fg62 significantly induced the expression of *NbPR1* and *NbPR2* (Fig. 6c).

Transcript levels of well-known PTI-related marker genes in *N. benthamiana* were also examined. Fg62 induced the expression of *NbCYP71D20* and *NbPia5* (Fig. 6d). Together, these results suggest that Fg62 is recognized by *N. benthamiana* and activates plant immunity.

Fg62 improves soybean resistance to *F. graminearum* and *P. sojae*

Next, we investigated the ability of Fg62 to induce disease resistance in soybean, which is the host of *F. graminearum* and *P. sojae*. We soaked soybean seeds in 1 μM Fg62 protein solution for 12 h, using buffer and GFP protein solution as experimental controls. Then the treated soybean seeds were seeded in vermiculite mixed with pathogen mycelium. After 10 days in a greenhouse, Fg62-treated soybeans were significantly resistant to *P. sojae* infection, with improved survival rate, fresh weight, and plant height compared to the controls (Fig. 7a–d). Similarly, soybeans soaked in Fg62 protein solution grew better in vermiculite mixed with *F. graminearum* than did the controls (Fig. 7e–h).

To investigate whether Fg62 had effect on pathogen growth, the three pathogens were cultured on medium containing Fg62 protein at a concentration of 1 μM. Fg62 had no effect on the colony morphology or growth rate of the three pathogens (Additional file 2: Figure S5). In conclusion, Fg62 enhanced plant resistance to multiple pathogens.

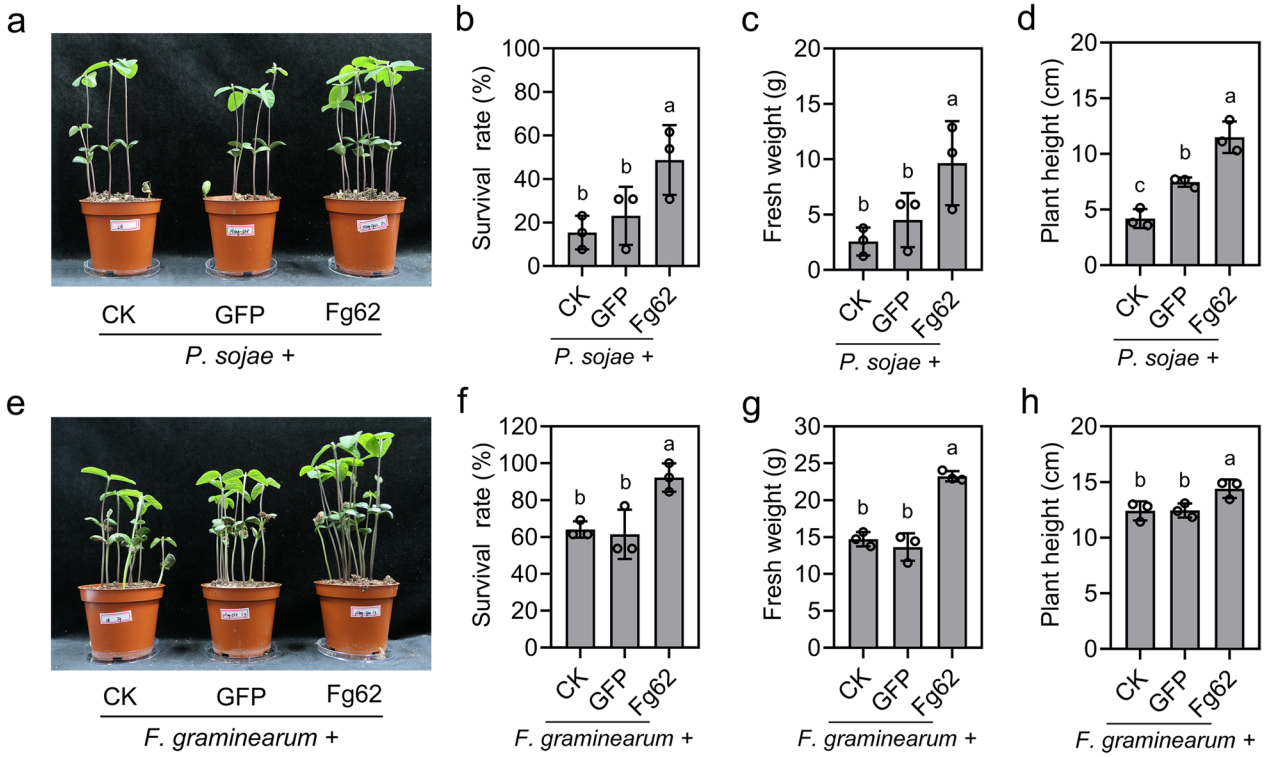

Fig. 7 Fg62 induces soybean resistance to *Phytophthora sojae* and *Fusarium graminearum*. **a**, **e** Representative photographs of soybean at 10 dpi under different treatments. Hefeng47 soybean seeds were soaked in protein solution or buffer for 12 h and then grown in sterilized vermiculite mixed with *P. sojae* or *F. graminearum* mycelium pieces. Each pot contained 15 soybean seeds and the experiment was repeated three times independently. Soybean survival rates (**b**, **f**), fresh weight (**c**, **g**), and plant heights (**d**, **h**) for **a** and **e**. Means and SEs from three independent experiments are shown. Asterisks indicate significant differences from the control based on Student's *t*-test

Discussion

F. graminearum is a hemibiotrophic fungus that does not cause visible symptoms in the initial infection stage because the infected hyphae grow in subcuticular and intercellular plant tissues (Brown et al. 2010; Walter et al. 2010). Hemibiotrophic pathogens such as *P. sojae* deliver apoplastic and intracellular effector proteins to modulate innate immunity in hosts (Wang and Wang 2018). The *F. graminearum* genome encodes large numbers of secreted effector proteins and may play roles in *F. graminearum*-host interactions (Lu and Edwards 2016). However, to date, only a handful of the effectors have been identified as contributing to virulence and affecting plant immunity. In addition, most secreted effector proteins have no predictable function (Presti et al. 2015).

In this study, we identified and functionally characterized a total of eight secretory proteins without predictable function from *F. graminearum* (Fig. 1 and Additional file 1: Table S1). Among these, only Fg62 triggered cell death, and this protein was selected for further characterization. Plant cell death is a universal phenomenon in plant-pathogen interactions, and has long been recognized as a hallmark of plant immunity (Xi et al. 2021).

Many proteins that induce cell death contain non-full-length functional regions or peptides that play critical roles in inducing cell death or activating plant immunity. For example, a 32-amino acid peptide of Fg02685 is sufficient for the induction of oxidative burst, callose deposition, and the activation of the mitogen-activated protein kinase signal in plants (Xu et al. 2022). An intra-molecular disulfide bond between C94 and C105 is important for the folding and stability of Osp24 protein, and these two cysteine residues are essential for its function (Jiang et al. 2020). Although Fg62 is dispensable for growth and the stress response, it is important for infectious growth in infected plants. Fg62 lacks a conserved domain but contains seven cysteine residues. Three putative intramolecular disulfide bonds were found in Fg62 using the DiANNA v1.1 web server (data not shown). Further research is needed to determine which disulfide bond has a more critical effect on the function of Fg62.

Fg62 was previously considered to be an orphan gene in *F. graminearum* (Jiang et al. 2020). Orphan genes are protein-coding regions that are restricted to a single species or narrow clade, with no recognizable homolog in distantly related species (Domazet-Loso and Tautz

2003). BLAST analysis identified homologous sequences to Fg62 only in *F. culmorum* and *F. pseudograminearum*, and the homologous proteins induced cell death in *N. benthamiana* (Fig. 5). *F. graminearum*, *F. culmorum*, and *F. pseudograminearum* are members of the *F. sambucinum* species complex, which contains the most important FHB pathogens affecting cereal crops worldwide (Kelly et al. 2016). The *F. graminearum* genome is predicted to encode hundreds of orphan proteins; however, their roles in the pathogenic interactions of plants via *F. graminearum* remain to be characterized. Osp24, an orphan secretory protein from *F. graminearum*, functions as a cytoplasmic effector that modulates host immunity by mediating proteasomal degradation of wheat SNF1-related kinase TaSnRK1α, which is specifically expressed during plant infection and is important for infectious growth (Jiang et al. 2020). Fg62 was identified from the *F. graminearum* secretome, and is specifically expressed during early infection (Fig. 2), suggesting that it is an extracellular effector. However, the functional position of Fg62, that is, whether it is attached to the fungal cell wall, resides in the apoplast, or can be transferred to plant cells, remains unknown at present.

In our agroinfiltration assays using *N. benthamiana* leaves, Fg62 showed delayed cell death induction, occurring after 7 days of treatment, significantly slower than that of the *P. sojae* extracellular effector PsXEG1 (Ma et al. 2015). Effector-mediated plant cell death may result from ETI or prolonged effects on its virulence targets. Effectors can also induce PTI following their recognition by plant PRRs, causing cell death. For example, RXEG1, a leucine-rich repeat receptor-like protein identified from *N. benthamiana*, can specifically recognize PsXEG1 (Wang et al. 2018). In this study, we found that the recombinant Fg62 protein activated typical plant PTI-related responses, as the induction of PTI-related marker genes (*NbCYP71D20* and *NbPia5*) by Fg62 was fivefold higher than that in the control group, suggesting that the cytotoxic effects of Fg62 are partly related to the PTI response. Fg62 protein also significantly induced expression of the plant defense-related genes *NbPR1* and *NbPR2*, which increased more than 30-fold (Fig. 6). However, whether the plant defense response induced by Fg62 is dependent on the conserved receptors BAK1 and SOBIR1, and the tangible immune activation mechanism of Fg62 require further exploration.

Excessive use of traditional fungicides leads to increased fungicide resistance in pathogens, as well as environmental pollution. Microbe elicitors are generally considered environmentally friendly biological reagents that enhance disease resistance in plants, and the potential future application of these green and nonpolluting agents appears promising. In this study, Fg62 was identified as an extracellular protein from *F. graminearum* that induces plant immunity. Treatment with recombinant Fg62 protein contributed to plant resistance against *P. capsici.* in *N. benthamiana*, *F. graminearum*, and *P. sojae* in soybean (Figs. 6, 7), indicating that Fg62 acts as a plant immune inducer to achieve disease control.

Conclusions

This study sheds light on the roles of *F. graminearum* secreted protein Fg62 which induces plant cell death and contributes to fungal virulence. The results indicate knockouting of *Fg62* reduce disease development in infected plant tissue. Fg62 enhances plant disease resistance against oomycetes and fungal pathogens as a plant immune inducer. This study provides a viable alternative to control crop diseases by exploiting induced plant resistance through the application of a novel bioactive immune inducer.

Methods

Biological materials and culture conditions

P. sojae strain P6497 and *P. capsici* strain LT263 were maintained on 10% vegetable juice medium (V8) at 25°C in the dark. The *F. graminearum* strain PH-1 and its mutants were cultured on potato dextrose agar medium (PDA) at 25°C. Mycelial growth of the *F. graminearum* WT strain PH-1 and the transformants was assayed on PDA, complete minimal medium (CM), and minimal medium (MM), and images were taken at three days after inoculation. To determine the sensitivity of the strains to various stresses, 5 mm mycelial plugs of each strain were sampled from a 3-day-old colony edge and inoculated on PDA supplemented with each stress agent at concentrations indicated in the figure captions. Three biological replicates were used for each strain and each experiment was repeated three times independently.

The soybean cultivar Hefeng47 was used for virulence assays. Seedlings were grown at 25°C under a 14 h/10 h day/night photoperiod. Etiolated hypocotyls harvested after growth at 25°C without light were used for *P. sojae* inoculations to produce infected tissue. *N. benthamiana* plants were grown in a greenhouse for 4–6 weeks at 25°C under a 14 h/10 h day/night photoperiod.

qRT-PCR analysis

Samples were collected and ground in liquid nitrogen. Total RNA was extracted using an RNA kit and cDNA synthesis was performed using a HiScript II 1st Strand cDNA Synthesis Kit. To evaluate pathogen biomass, the gDNA of pathological tissue was used as a template for uniform concentration.

qRT-PCR was conducted in a 20 μL reaction mix containing 20 ng gDNA, 0.4 μL primers (10 μM) specific for the target or reference gene, 10 μL SYBR Green Premix Ex Taq, 0.4 μL ROX Reference Dye II (50×), and 6.8 μL sterilized deionized water. qRT-PCR was run on the Applied Biosystems 7500 Real Time PCR System under the following conditions: 95°C for 30 s, followed by 40 cycles at 95°C for 5 s and 60°C for 34 s, dissociation at 95°C for 15 s, 60°C for 1 min, and 95°C for 15 s. Mean Ct values were subjected to normalization.

Gene deletion and complementation

F. graminearum gene deletion mutants were constructed using a polyethylene glycol-mediated protoplast transformation method. Fresh mycelia cultured in yeast extract-peptone-dextrose growth medium (YEPD) were treated with driselase and lysing enzymes to obtain *Fusarium* protoplasts. The primers used to amplify the flanking sequences are listed in Additional file 1: Table S3. The complement fragments containing the native promoter region and the entire coding region, obtained by double-joint PCR, were co-transformed with XhoI-digested pYF11 (R25001; Thermo Fisher Scientific, USA) into the yeast strain XK1-25 using the Alkali-Cation TM Yeast Transformation Kit (MP Biomedicals) to generate an Fg62-GFP fusion vector. Complement vectors were transformed into mutant protoplasts and screened for geneticin resistance.

Functional verification of Fg62 signal peptide

The predicted N-terminal 19-amino acid SP sequence of Fg62 was fused in frame to the invertase gene in the pSUC2 vector, which carries the sucrose invertase gene *SUC2* without the initiation ATG codon and was transformed into yeast YTK12. *EcoRI* and *XhoI* restriction enzymes were used to insert the SP sequences into the pSUC2 vector. The transformant strains were then screened on YPDA, CMD-W plates and selective YPRAA plates. YTK12 strains with empty pSUC vector or pSUC2-Avr1bSP were used as the negative and positive controls, respectively. The enzymatic activity was tested by reducing 2,3,5-triphenyl tetrazolium chloride to red 1,3,5-triphenyl formazan.

For localization in *N. benthamiana*, full-length Fg62 and Fg62-nsp tagged with GFP were transformed into *Agrobacterium tumefaciens*, and the bacterial suspension with $OD_{600}=0.6$ were injected into 4-week-old *N. benthamiana* leaves. At 36 hpi, patches of agroinfiltrated leaves were cut and treated with 70 mM NaCl for 10 min, then analyzed using an LSM 710 laser scanning microscope (Carl Zeiss, Germany) (Xia et al. 2020).

Agroinfiltration assays

Fragments used to generate overexpression constructs were amplified by PCR with 2× Phanta Max Master Mix (Vazyme Biotech, China), and cDNA of *F. graminearum* or different *Fusarium* species served as a template. The primers used are listed in Additional file 1: Table S3. The purified fragments were cloned into the modified vector pGR107-HA using the ClonExpress Ultra One Step Cloning Kit (Vazyme Biotech, China). The constructed vector was transferred into *Escherichia coli*. Plasmids were obtained through *E. coli* culture and then transferred into *A. tumefaciens* strain GV3101.

A. tumefaciens strain GV3101 was grown overnight at 28°C in lysogeny broth (LB) medium containing the appropriate antibiotics. For agroinfiltration assays, *A. tumefaciens* cells were resuspended in infiltration buffer (10 mM $MgCl_2$, 1 mM MES at pH 5.6, and 200 μM acetosyringone). Leaves of 4-week-old *N. benthamiana* were used for infiltration.

Extraction of transiently expressed proteins

N. benthamiana leaves were collected at 48 h after agroinfiltration and ground in liquid nitrogen. Proteins were extracted using lysis buffer (1% Triton X-100, Beyotime Biotechnology, China) containing a protease inhibitor cocktail (Sigma-Aldrich, USA). The samples were centrifuged at 4°C for 15 min at 14,000 *g* and then boiled in protein sample buffer for 10 min. Subsequently, proteins were analyzed by sodium dodecyl sulfate–polyacrylamide gel electrophoresis (SDS-PAGE) and immunoblotting.

Prokaryotic expression and purification of recombinant Fg62 protein

For prokaryotic expression in *E. coli*, *Fg62* coding sequence was inserted into the pGEX-4 T-2 vector, which was transformed into *E. coli* BL21 and cultured overnight at 37°C in LB medium. Subsequently, *E. coli* cells were diluted (1:50) in fresh LB medium and grown at 37°C to an optical density (OD) of 0.6. Recombinant protein expression was induced with 0.1 mM isopropyl β-d-1-thiogalactopyranoside (IPTG) for 12 h at 20°C. *E. coli* cells were precipitated by high-speed centrifugation and homogenized using a high-pressure homogenizer. Recombinant proteins were purified using the AKTA Avant 25 system (GE Healthcare, UK) with GST-Sep Glutathione 4FF Chromatography Columns (5 mL, G1827651) and HiTrap 26/10 Desalting Prepacked Columns (10262891). The proteins were concentrated using ultrafiltration tubes (Amicon Ultra, Ultracel-10 K, Millipore, USA). Protein concentrations were determined using the BCA Protein Assay Kit (Solarbio, China).

Pathogenicity assay

Etiolated soybean hypocotyls were inoculated with 1.5 cm diameter medium blocks containing 3-day-old pathogen mycelia. The inoculated seedlings were maintained in a greenhouse at 25°C under a 14 h/10 h light/dark cycle. Pathogen virulence was analyzed after 3 days.

Wheat cultivar NJ58 was used for coleoptile infection. Seeds were randomly planted and cultivated at 25°C under a 14 h/10 h light/dark cycle. We inoculated 2 μL spore suspension (10^6/mL) onto wheat coleoptiles. Lesion sizes on the coleoptiles were measured at 7 dpi.

For potted soybean inoculation, *F. graminearum* PH-1 and *P. sojae* P6497 were grown in 9 cm Petri dishes containing 15 mL medium and cultured for 6–8 days at 25°C. Then the medium was chopped and mixed with vermiculite, and four dishes of medium were added to each pot. Soybean seeds were soaked in protein solution or buffer for 12 h and then grown in sterilized vermiculite mixed with mycelium pieces and maintained in a greenhouse for 10 days at 25°C under a 14 h/10 h light/dark cycle.

DON production assays

For DON production assays, all strains were grown in liquid trichothecene biosynthesis (TBI) medium at 28°C for 7 days in the dark, and then liquid and mycelia were collected respectively (Zheng et al. 2018). Liquid DON production was determined using a DON ELISA Assay Kit (Wise, China), mycelia were dried and weight for quantification.

Bioinformatics analysis

Signal peptide prediction was performed using the SignalP-5.0 server (http://www.cbs.dtu.dk/services/SignalP/). The ApoplastP machine learning model (https://apoplastp.csiro.au/) was used to predict subcellular-localization.

A phylogenetic tree was constructed using the neighbor-joining method in the MEGA X software based on the protein sequences. The percentages of replicate trees in which associated taxa clustered together in the bootstrap test (1000 replicates) were calculated. The tree was drawn to scale, with branch lengths in the same units as those of the evolutionary distances used to infer the tree. Evolutionary distances were computed using the Poisson correction method and are expressed as numbers of amino acid substitutions per site.

All experiments were performed at least three times. The GraphPad Prism software was used to perform the statistical analysis and draw the figures.

Abbreviations

DON	Deoxynivalenol
ETI	Effector-triggered immunity
FHB	Fusarium head blight
GFP	Green fluorescent protein
NLRs	Nucleotide binding-domain, leucine-rich, repeat-containing receptors
PAMPs	Pathogen-associated molecular patterns
PRRs	Pattern recognition receptors
PTI	PAMP-triggered immunity
ROS	Reactive oxygen species
SPs	Signal peptides

Supplementary Information

The online version contains supplementary material available at https://doi.org/10.1186/s42483-023-00167-z.

Additional file 1: **Table S1**. 12 candidate proteins from the *Fusarium graminearum* secretome. **Table S2**. DON production of different strains. **Table S3**. Primers used in this study.

Additional file 2: **Figure S1**. Knocking out Fg62 in *Fusarium graminearum*. **Figure S2**. Fg62 had no effect on the growth of *Fusarium graminearum*. **Figure S3**. Fg62 had no effect on sensitivity to multiple stresses of *Fusarium graminearum*. **Figure S4**. Prokaryotic expression and purification of Fg62. **Figure S5**. Recombinant Fg62 protein had no effect on pathogen growth.

Acknowledgements

Not applicable.

Authors' contributions

YW, XZ, WY, and BY conceived the experiments; SW, SY, KD, WZ, and XZ performed the experiments; SW, SY, and WY analyzed the data; SW, SY, and BY wrote the manuscript. All authors read and approved the final manuscript.

Funding

This work was supported by Grants from the National Natural Science Foundation of China (32001882, 32172374, and 31721004).

Availability of data and materials

Not applicable.

Declarations

Ethics approval and consent to participate

Not applicable.

Consent for publication

Not applicable.

Competing interests

The authors declare that they have no competing interests.

Received: 4 November 2022 Accepted: 8 February 2023
Published online: 04 April 2023

References

Audenaert K, Vanheule A, Höfte M, Haesaert G. Deoxynivalenol: a major player in the multifaceted response of *Fusarium* to its environment. Toxins. 2013;6:1–19. https://doi.org/10.3390/toxins6010001.

Boller T, Felix G. A renaissance of elicitors: perception of microbe-associated molecular patterns and danger signals by pattern-recognition receptors.

Annu Rev Plant Biol. 2009;60:379–406. https://doi.org/10.1146/annurev.arplant.57.032905.105346.
Broders KD, Lipps PE, Paul PA, Dorrance AE. Evaluation of *Fusarium graminearum* associated with corn and soybean seed and seedling disease in Ohio. Plant Dis. 2007;91:1155–60. https://doi.org/10.1094/pdis-91-9-1155.
Brown NA, Urban M, van de Meene AM, Hammond-Kosack KE. The infection biology of *Fusarium graminearum*: defining the pathways of spikelet to spikelet colonisation in wheat ears. Fungal Biol. 2010;114:555–71. https://doi.org/10.1016/j.funbio.2010.04.006.
Chang XL, Dai H, Wang DP, Zhou HH, He WQ, Fu Y, et al. Identification of *Fusarium* species associated with soybean root rot in Sichuan Province. China Eur J Plant Pathol. 2018;151:563–77. https://doi.org/10.1007/s10658-017-1410-7.
Couto D, Zipfel C. Regulation of pattern recognition receptor signalling in plants. Nat Rev Immunol. 2016;16:537–52. https://doi.org/10.1038/nri.2016.77.
Dean R, Van Kan JA, Pretorius ZA, Hammond-Kosack KE, Di Pietro A, Spanu PD, et al. The Top 10 fungal pathogens in molecular plant pathology. Mol Plant Pathol. 2012;13:414–30. https://doi.org/10.1111/j.1364-3703.2011.00783.x.
Domazet-Loso T, Tautz D. An evolutionary analysis of orphan genes in *Drosophila*. Genome Res. 2003;13:2213–9. https://doi.org/10.1101/gr.1311003.
Duplessis S, Cuomo CA, Lin Y-C, Aerts A, Tisserant E, Veneault-Fourrey C, et al. Obligate biotrophy features unraveled by the genomic analysis of rust fungi. Proc Natl Acad Sci USA. 2011;108:9166–71. https://doi.org/10.1073/pnas.1019315108.
Giraldo MC, Valent B. Filamentous plant pathogen effectors in action. Nat Rev Microbiol. 2013;11:800–14. https://doi.org/10.1038/nrmicro3119.
Jiang C, Hei R, Yang Y, Zhang S, Wang Q, Wang W, et al. An orphan protein of *Fusarium graminearum* modulates host immunity by mediating proteasomal degradation of TaSnRK1α. Nat Commun. 2020;11:4382. https://doi.org/10.1038/s41467-020-18240-y.
Jones JDG, Dangl JL. The plant immune system. Nature. 2006;444:323–9. https://doi.org/10.1038/nature05286.
Kelly A, Proctor RH, Belzile F, Chulze SN, Clear RM, Cowger C, et al. The geographic distribution and complex evolutionary history of the NX-2 trichothecene chemotype from *Fusarium graminearum*. Fungal Genet Biol. 2016;95:39–48. https://doi.org/10.1016/j.fgb.2016.08.003.
Li G, Zhou J, Jia H, Gao Z, Fan M, Luo Y, et al. Mutation of a histidine-rich calcium-binding-protein gene in wheat confers resistance to Fusarium head blight. Nat Genet. 2019;51:1106–12. https://doi.org/10.1038/s41588-019-0426-7.
Lu S, Edwards MC. Genome-wide analysis of small secreted cysteine-rich proteins identifies candidate effector proteins potentially involved in *Fusarium graminearum*-wheat interactions. Phytopathology. 2016;106:166–76. https://doi.org/10.1094/phyto-09-15-0215-r.
Ma LJ, Geiser DM, Proctor RH, Rooney AP, O'Donnell K, Trail F, et al. *Fusarium* pathogenomics. Annu Rev Microbiol. 2013;67:399–416. https://doi.org/10.1146/annurev-micro-092412-155650.
Ma ZC, Song TQ, Zhu L, Ye WW, Wang Y, Shao YY, et al. A *Phytophthora sojae* glycoside hydrolase 12 Protein is a major virulence factor during soybean infection and is recognized as a PAMP. Plant Cell. 2015;27:2057–72. https://doi.org/10.1105/tpc.15.00390.
Ngou BPM, Ahn HK, Ding P, Jones JDG. Mutual potentiation of plant immunity by cell-surface and intracellular receptors. Nature. 2021;592:110–5. https://doi.org/10.1038/s41586-021-03315-7.
O'Donnell K, Rooney AP, Proctor RH, Brown DW, McCormick SP, Ward TJ, et al. Phylogenetic analyses of RPB1 and RPB2 support a middle Cretaceous origin for a clade comprising all agriculturally and medically important fusaria. Fungal Genet Biol. 2013;52:20–31. https://doi.org/10.1016/j.fgb.2012.12.004.
Peng Y, van Wersch R, Zhang Y. Convergent and divergent signaling in PAMP-triggered immunity and effector-triggered immunity. Mol Plant Microbe Interact. 2018;31:403–9. https://doi.org/10.1094/mpmi-06-17-0145-cr.
Pioli RN, Mozzoni L, Morandi EN. First report of pathogenic association between *Fusarium graminearum* and soybean. Plant Dis. 2004;88:220. https://doi.org/10.1094/pdis.2004.88.2.220a.
Presti LL, Lanver D, Schweizer G, Tanaka S, Liang L, Tollot M, et al. Fungal effectors and plant susceptibility. Annu Rev Plant Biol. 2015;66:513–45. https://doi.org/10.1146/annurev-arplant-043014-114623.
Pruitt RN, Locci F, Wanke F, Zhang L, Saile SC, Joe A, et al. The EDS1-PAD4-ADR1 node mediates *Arabidopsis* pattern-triggered immunity. Nature. 2021;598:495–9. https://doi.org/10.1038/s41586-021-03829-0.
Qi PF, Zhang YZ, Liu CH, Chen Q, Guo ZR, Wang Y, et al. Functional analysis of FgNahG clarifies the contribution of salicylic acid to wheat (*Triticum aestivum*) resistance against *Fusarium* head blight. Toxins. 2019. https://doi.org/10.3390/toxins11020059.
Starkey DE, Ward TJ, Aoki T, Gale LR, Kistler HC, Geiser DM, et al. Global molecular surveillance reveals novel *Fusarium* head blight species and trichothecene toxin diversity. Fungal Genet Biol. 2007;44:1191–204. https://doi.org/10.1016/j.fgb.2007.03.001.
Stergiopoulos I, Collemare J, Mehrabi R, De Wit PJ. Phytotoxic secondary metabolites and peptides produced by plant pathogenic *Dothideomycete* fungi. FEMS Microbiol Rev. 2013;37:67–93. https://doi.org/10.1111/j.1574-6976.2012.00349.x.
Stergiopoulos I, de Wit PJ. Fungal effector proteins. Annu Rev Phytopathol. 2009;47:233–63. https://doi.org/10.1146/annurev.phyto.112408.132637.
Su Z, Bernardo A, Tian B, Chen H, Wang S, Ma H, et al. A deletion mutation in *TaHRC* confers *Fhb1* resistance to *Fusarium* head blight in wheat. Nat Genet. 2019;51:1099–105. https://doi.org/10.1038/s41588-019-0425-8.
Tsuda K, Katagiri F. Comparing signaling mechanisms engaged in pattern-triggered and effector-triggered immunity. Curr Opin Plant Biol. 2010;13:459–65. https://doi.org/10.1016/j.pbi.2010.04.006.
Voigt CA, Schäfer W, Salomon S. A secreted lipase of *Fusarium graminearum* is a virulence factor required for infection of cereals. Plant J. 2005;42:364–75. https://doi.org/10.1111/j.1365-313X.2005.02377.x.
Walter S, Nicholson P, Doohan FM. Action and reaction of host and pathogen during *Fusarium* head blight disease. New Phytol. 2010;185:54–66. https://doi.org/10.1111/j.1469-8137.2009.03041.x.
Wang H, Sun S, Ge W, Zhao L, Hou B, Wang K, et al. Horizontal gene transfer of *Fhb7* from fungus underlies Fusarium head blight resistance in wheat. Science. 2020. https://doi.org/10.1126/science.aba5435.
Wang Y, Wang Y. *Phytophthora sojae* effectors orchestrate warfare with host immunity. Curr Opin Microbiol. 2018;46:7–13. https://doi.org/10.1016/j.mib.2018.01.008.
Wang Y, Xu Y, Sun Y, Wang H, Qi J, Wan B, et al. Leucine-rich repeat receptor-like gene screen reveals that *Nicotiana* RXEG1 regulates glycoside hydrolase 12 MAMP detection. Nat Commun. 2018;9:594. https://doi.org/10.1038/s41467-018-03010-8.
Xi Y, Chochois V, Kroj T, Cesari S. A novel robust and high-throughput method to measure cell death in *Nicotiana benthamiana* leaves by fluorescence imaging. Mol Plant Pathol. 2021;22:1688–96. https://doi.org/10.1111/mpp.13129.
Xia Y, Ma Z, Qiu M, Guo B, Zhang Q, Jiang H, et al. N-glycosylation shields *Phytophthora sojae* apoplastic effector PsXEG1 from a specific host aspartic protease. Proc Natl Acad Sci USA. 2020;117:27685–93. https://doi.org/10.1073/pnas.2012149117.
Xu Q, Hu S, Jin M, Xu Y, Jiang Q, Ma J, et al. The N-terminus of a *Fusarium graminearum*-secreted protein enhances broad-spectrum disease resistance in plants. Mol Plant Pathol. 2022;23:1751–64. https://doi.org/10.1111/mpp.13262.
Yang B, Wang Y, Tian M, Dai K, Zheng W, Liu Z, et al. Fg12 ribonuclease secretion contributes to *Fusarium graminearum* virulence and induces plant cell death. J Integr Plant Biol. 2021;63:365–77. https://doi.org/10.1111/jipb.12997.
Ye W, Zeng D, Xu M, Yang J, Ma J, Wang Y, et al. A LAMP-assay-based specific microbiota analysis reveals community dynamics and potential interactions of 13 major soybean root pathogens. J Integr Agric. 2020;19:2056–63. https://doi.org/10.1016/s2095-3119(19)62855-8.
Yuan M, Jiang Z, Bi G, Nomura K, Liu M, Wang Y, et al. Pattern-recognition receptors are required for NLR-mediated plant immunity. Nature. 2021a;592:105–9. https://doi.org/10.1038/s41586-021-03316-6.
Yuan M, Ngou BPM, Ding P, Xin XF. PTI-ETI crosstalk: an integrative view of plant immunity. Curr Opin Plant Biol. 2021b;62:102030. https://doi.org/10.1016/j.pbi.2021.102030.
Yulfo-Soto G, Smith HS, Szarka D, Dixon E, Vaillancourt L, Gauthier N. First report of *Fusarium graminearum* causing flower blight on hemp (*Cannabis sativa*) in Kentucky. Plant Dis. 2022;106:334. https://doi.org/10.1094/pdis-06-21-1292-pdn.
Zheng H, Li L, Miao P, Wu C, Chen X, Yuan M, et al. FgSec2A, a guanine nucleotide exchange factor of FgRab8, is important for polarized growth,

pathogenicity and deoxynivalenol production in *Fusarium graminearum*. Environ Microbiol. 2018;20:3378–92. https://doi.org/10.1111/1462-2920.14373.

Zuccaro A, Lahrmann U, Güldener U, Langen G, Pfiffi S, Biedenkopf D, et al. Endophytic life strategies decoded by genome and transcriptome analyses of the mutualistic root symbiont *Piriformospora indica*. PLoS Pathog. 2011;7:e1002290. https://doi.org/10.1371/journal.ppat.1002290.